UNIVERSITY POLITEHNICA OF BUCHAREST
FACULTY OF BIOTECHNICAL SYSTEMS ENGINEERING

Doctoral school: Biotechnical Engineering

Senate number … from …./2018

Summary

THESIS FOR DEGREE OF DOCTOR OF PHILOSOPHY

"Contribution to Kinematic and Dynamic Study of Rigid Bodies"

PhD Student: Ing. NGUYEN THIEN VAN
PhD Supervisor: Prof. dr. ing. ION STROE

PhD COMMISSION

President	Prof. dr. ing. DAVID LADISLAU	Faculty of biotechnical engineering-UPB
PhD Supervisor	Prof. dr. ing. Ion STROE	Faculty of biotechnical engineering-UPB
Reviewer	Prof. dr. ing. Andrei CRAIFALEANU	Faculty of biotechnical engineering-UPB
Reviewer	CS1, dr.ing. Achim IONITA	INCAS-Bucharest
Reviewer	Prof. dr. ing. Dinel POPA	Pitesti University

BUCHAREST 2018

Contents

1. Abstract

This thesis presented a new method to determine directly internal forces in a rigid body of multibody systems or in a group of links having relative translation with each other based on Lagrange equations. With this method, we can avoid difficulties that previous methods encounter during computational process by without considering constraint forces appearing in connected joints between links of the multibody systems.

By using a set of generalized coordinates that is consistent with constraint relations and describes completely configuration of the mechanism, we can establish the differential equations governing the motion of system. In addition, by introducing a supplementary mobility we can compute directly the internal force corresponding to that mobility thanks to the principle: If an internal force is found, a corresponding supplementary mobility is considered in the system. After forming the differential equation for the new mobility, the internal force will be determined via the equation by imposing null values of the mobility as well as its first and second derivatives.

For illustrating proposed method, some commonly used mechanisms are chosen as models to analyze. They are planar mechanisms and spatial mechanism. With planar mechanisms, the slider-crank and the system for controlling aircraft elevator are considered. In there, the internal forces are computed in the links having general plane motion (the connecting rod in the slider-mechanism, and the subsystem hydraulic cylinder for the other). And a 3-DOF articulated manipulator is considered to analyze for the case of spatial mechanism. For this case, internal forces in the end-effector are determined.

Finally, the thesis also applies some fundamental definition of controlling theory and Genetic Algorithms (GAs) in tuning parameters of PID controllers to control a 4-DOF spatial mechanism, that the end-effector of the mechanism is imposed to follow a defined trajectory. Based on that, the Algorithm can be used and developed for simulating model robots in designed step.

2. Kinematics and Dynamics of rigid bodies system

2.1. Determining linear velocity of a point of rigid body in the mechanism

Supposing we have a set of reference systems $O_0x_0y_0z_0$, $O_1x_1y_1z_1$,…, $O_ix_iy_iz_i$,…, $O_nx_ny_nz_n$ as shown in the Figure 1. Determining position of an arbitrary point P_i on a rigid body (B_i) attached a reference frame $O_ix_iy_iz_i$ in the base frame $O_0x_0y_0z_0$ through pre-adjacent links, which can be specified about positions and orientations, is presented as following:

From geometrical relations, we can write:

$$\begin{aligned}
&\overrightarrow{O_0P_i}_{(0)} = \overrightarrow{O_0O_1}_{(0)} + \overrightarrow{O_1P_i}_{(1)}, \\
&\overrightarrow{O_1P_i}_{(1)} = \overrightarrow{O_1O_2}_{(1)} + \overrightarrow{O_2P_i}_{(2)}, \\
&\overrightarrow{O_2P_i}_{(2)} = \overrightarrow{O_2O_3}_{(2)} + \overrightarrow{O_3P}_{i(3)}, \\
&\dots\dots\dots\dots\dots\dots \\
&\overrightarrow{O_{i-1}P_i}_{(i-1)} = \overrightarrow{O_{i-1}O_i}_{(i-1)} + \overrightarrow{O_iP}_{i(i)}.
\end{aligned} \tag{1}$$

Replacing successively all expressions of $\overrightarrow{O_1P_i}_{(1)}, \overrightarrow{O_2P_i}_{(2)}, \overrightarrow{O_3P_i}_{(3)}, \dots, \overrightarrow{O_{i-1}P_i}_{(i-1)}$ into the pre-adjacent expressions, and finally into the expression of $\overrightarrow{O_0P_i}_{(0)}$, yielded:

$$\overrightarrow{O_0P_i}_{(0)} = \overrightarrow{O_0O_1}_{(0)} + \overrightarrow{O_1O_2}_{(1)} + \overrightarrow{O_2O_3}_{(2)} + \dots + \overrightarrow{O_{i-1}O_i}_{(i-1)} + \overrightarrow{O_iP_i}_{(i)}, \tag{2}$$

where $\overrightarrow{O_{k-1}O_k}_{(k-1)}$ is the vector giving position of the origin O_k in the reference frame $O_{k-1}x_{k-1}y_{k-1}z_{k-1}$ (with k=1, 2,…, i),

$\overrightarrow{O_iP_i}_{(i)}$ is the vector giving position of the point P_i in the reference frame $O_ix_iy_iz_i$.

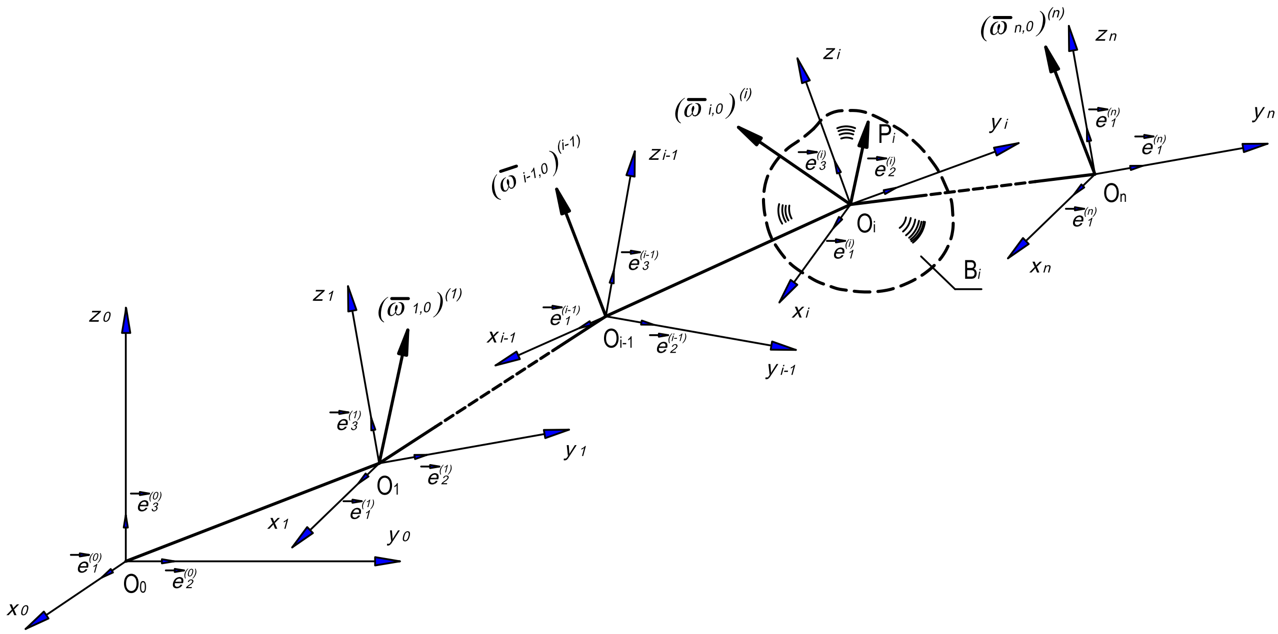

Figure 1. The system of reference frames in space

If we express the position of P_i in the base frame $O_0x_0y_0z_0$ in the matrix form, then Eq. (2) can be rewritten as below:

$$\begin{aligned}\{O_0P_i\}_{(0)} &= [I].\{O_0O_1\}_{(0)} + {}_1^0[R].\{O_1O_2\}_{(1)} + {}_2^0[R].\{O_2O_3\}_{(2)} + \\ &+ {}_3^0[R].\{O_3O_4\}_{(3)} + \ldots + {}_{i-1}^{\;\;0}[R].\{O_{i-1}O_i\}_{(i-1)} + {}_i^0[R].\{O_iP_i\}_{(i)},\end{aligned} \tag{3}$$

Or in the generalized form

$$\{O_0P_i\}_{(0)} = [I].\{O_0O_1\}_{(0)} + \sum_{k=2}^{i} {}_{k-1}^{\;\;0}[R].\{O_{k-1}O_k\}_{(k-1)} + {}_i^0[R].\{O_iP_i\}_{(i)}\ , \tag{4}$$

where $[I]$ is the 3×3 identity matrix,

${}_k^0[R]$ is the transformation matrix giving the orientation of the reference frame $O_kx_ky_kz_k$ relative to the base reference frame $O_0x_0y_0z_0$ (with k=1, 2,…, i).

And the linear velocity of the point P_i with respect to the base frame $O_0x_0y_0z_0$ is determined by carrying out the derivative versus time of Eq. (4), we obtained

$$\begin{aligned}\{V_{Pi}\}_{(0)} &= \frac{d}{dt}\left(\{O_0P_i\}_{(0)}\right) = [I].\frac{d}{dt}\left(\{O_0O_1\}_{(0)}\right) + \\ &+ \sum_{k=2}^{i}\left({}_{k-1}^{\;\;0}[\dot{R}].\{O_{k-1}O_k\}_{(k-1)} + {}_{k-1}^{\;\;0}[R].\frac{d}{dt}\left(\{O_{k-1}O_k\}_{(k-1)}\right)\right) + , \\ &+ {}_i^0[\dot{R}].\{O_iP_i\}_{(i)} + {}_i^0[R].\frac{d}{dt}\left(\{O_iP_i\}_{(i)}\right)\end{aligned} \tag{5}$$

2.2. Determining angular velocity of a rigid body in the mechanism

Considering again the body (B_i) attached rigidly a reference frame $O_ix_iy_iz_i$ as shown in Figure 1. Based on pre-adjacent links (B_{i-1}) (i=1,2…,n) in the mechanism, the angular velocity vector $\vec{\omega}_{i,0}$ is written in the form of matrix as

$$\{\omega_{i,0}\}_{(i)} = {}_{i-1}^{\;\;i}[R].\{\omega_{i-1,0}\}_{(i-1)} + \{\omega_{i,i-1}\}_{(i)}, \tag{6}$$

Similarly, we can write formula defining angular velocities for the others

$$
\begin{aligned}
&\{\omega_{i-1,0}\}_{(i-1)} = {}^{i-1}_{i-2}[R].\{\omega_{i-2,0}\}_{(i-2)} + \{\omega_{i-1,i-2}\}_{(i-1)} \\
&\{\omega_{i-2,0}\}_{(i-2)} = {}^{i-2}_{i-3}[R].\{\omega_{i-3,0}\}_{(i-3)} + \{\omega_{i-2,i-3}\}_{(i-2)}, \\
&\ldots\ldots\ldots\ldots\ldots\ldots\ldots\ldots\ldots\ldots\ldots\ldots \\
&\{\omega_{2,0}\}_{(2)} = {}^{2}_{1}[R].\{\omega_{1,0}\}_{(1)} + \{\omega_{2,1}\}_{(2)} \\
&\{\omega_{1,0}\}_{(1)} = [I].\{\omega_{1,0}\}_{(1)}
\end{aligned}
\tag{7}
$$

Replacing successively the post-expressions into pre-expressions from relations (6), (7), finally we obtained the generalized form determining the angular velocity of the body (B_i) in matrix form as following

$$\{\omega_{i,0}\}_{(i)} = \sum_{k=1}^{i-1} {}^{i}_{k}[R].\{\omega_{k,k-1}\}_{(k)} + \{\omega_{i,i-1}\}_{(i)}, \tag{8}$$

where ${}^{k}_{k-1}[R]$ is the transformation matrix giving the orientation of the reference frame $O_{k-1}x_{k-1}y_{k-1}z_{k-1}$ relative to the reference frame $O_kx_{kk}y_kz_k$ (with k=1, 2,…, i),

$\{\omega_{k,k-1}\}_{(k)}$ is the angular velocity vector of the body (B_k) relative to the body (B_{k-1}) and is defined in the reference frame $O_kx_{kk}y_kz_k$ (with k=1, 2,…, i),

$\{\omega_{i,0}\}_{(i)}$ is the angular velocity vector of the body (B_i) with respect to the base frame and is measured in the body frame $O_ix_iy_iz_i$,

${}^{i}_{k}[R]$ is the transformation matrix giving the orientation of the reference frame $O_kx_ky_kz_k$ relative to the reference frame $O_ix_{ik}y_iz_i$ (with k=1, 2,…, i-1) and is computed as

$${}^{i}_{k}[R] = {}^{i}_{i-1}[R].{}^{i-1}_{i-2}[R]\ldots{}^{k+1}_{k}[R], \tag{9}$$

And from Eq. (8) we can write the generalized form determining the angular velocity of the body (B_i) expressed in the base frame $O_0x_0y_0z_0$. By multiplying both sides of Eq. (8) with ${}^{0}_{i}[R]$, we have

$${}^{0}_{i}[R].\{\omega_{i,0}\}_{(i)} = \sum_{k=1}^{i-1} {}^{0}_{i}[R].{}^{i}_{k}[R].\{\omega_{k,k-1}\}_{(k)} + {}^{0}_{i}[R].\{\omega_{i,i-1}\}_{(i)}, \tag{10}$$

Or

$$\{\omega_{i,0}\}_{(0)} = \sum_{k=1}^{i-1} {}^{0}_{k}[R].\{\omega_{k,k-1}\}_{(k)} + \{\omega_{i,i-1}\}_{(0)}, \tag{11}$$

where $\{\omega_{i,0}\}_{(0)}$ is the angular velocity of the body (B_i) expressed in the reference frame $O_0x_{0k}y_0z_0$.

${}^{0}_{k}[R]$is the transformation matrix giving the orientation of the reference frame $O_kx_ky_kz_k$ relative to the base frame $O_0x_{0k}y_0z_0$ (with k=1, 2,…, i-1) and is computed as

$${}^{0}_{k}[R] = {}^{0}_{1}[R].{}^{1}_{2}[R]\ldots{}^{k-1}_{k}[R], \tag{12}$$

2.3. Equations of motion of rigid bodies system

As known, based on deriving equations of motion of particles system, Lagrange equations can be applied for a rigid bodies system.

For a non-holonomic system, the Lagrange equations corresponding to a system of n generalized coordinates

$$\frac{\mathrm{d}}{\mathrm{d}t}\left(\frac{\partial E}{\partial \dot{q}_j}\right)-\frac{\partial E}{\partial q_j}=Q_j+\sum_{i=1}^{n_C}\lambda_i a_{ij}\ ,\ (j=1,2,\ldots,n), \tag{13}$$

are completed with the n_C constraints

$$C_i(\dot{\vec{q}},\vec{q},t)=0\ ,\ (i=1,2,\ldots,n_C), \tag{14}$$

in there, $a_{ij}=\dfrac{\partial C_i}{\partial q_j}$ is coefficient of the multiplier λ_i.

For holonomic system, the constraints are written as following

$$C_i(\vec{q},t)=0\ ,\ (i=1,2,\ldots,n_C), \tag{15}$$

Then equations of motion for holonomic system of rigid bodies have expression as

$$\frac{\mathrm{d}}{\mathrm{d}t}\left(\frac{\partial E}{\partial \dot{q}_j}\right)-\frac{\partial E}{\partial q_j}=Q_j+\frac{\partial}{\partial q_j}\sum_{i=1}^{n_C}\lambda_i C_i,\ (j=1,2,\ldots,n), \tag{16}$$

By defining the analytical function

$$U=\sum_{i=1}^{n_C}\lambda_i C_i\ , \tag{17}$$

Eq. (16) can be written in the form

$$\frac{\mathrm{d}}{\mathrm{d}t}\left(\frac{\partial E}{\partial \dot{q}_j}\right)-\frac{\partial E}{\partial q_j}=Q_j+\frac{\partial U}{\partial q_j},\ (j=1,2,\ldots,n), \tag{18}$$

Starting from these n differential equations and using n_C relations of constraints, the generalized coordinates q_j and the Lagrange multipliers λ_i are determined.

2.4. Method for calculus of internal forces

For a mechanical system with n degrees of freedom represented by the independent generalized coordinates q_j (j=1,2…, n) , the Lagrange equations are expressed as following

$$\frac{\mathrm{d}}{\mathrm{d}t}\left(\frac{\partial E}{\partial \dot{q}_j}\right)-\frac{\partial E}{\partial q_j}=\frac{\partial U}{\partial q_j}+Q_j^*,\ (j=1,2,\ldots,n), \tag{19}$$

An internal force Q_{n+1}, as the new generalized force, can be found if a new fictitious mobility according to the force is considered. Then the mechanical system becomes one with (n+1) degrees of freedom. The equation for the new mobility is

$$\frac{\mathrm{d}}{\mathrm{d}t}\left(\frac{\partial E}{\partial \dot{q}_{n+1}}\right)-\frac{\partial E}{\partial q_{n+1}}=\frac{\partial U}{\partial q_{n+1}}+Q_{n+1}, \tag{20}$$

Considering again the mechanism, the internal force $\Re_{n+1}$ is easily obtained from Eq. (20) in the form

$$\Re_{n+1}=\left[\frac{\mathrm{d}}{\mathrm{d}t}\left(\frac{\partial E}{\partial \dot{q}_{n+1}}\right)-\frac{\partial E}{\partial q_{n+1}}-\frac{\partial U}{\partial q_{n+1}}\right]_{\substack{q_{n+1}=0\\ \dot{q}_{n+1}=0\\ \ddot{q}_{n+1}=0}}, \tag{21}$$

3. Calculus of internal forces in planar mechanisms

3.1. Calculating internal forces in an element of mechanism

Let consider a slider-crank mechanism as the rigid bodies system with one degree of freedom shown in Figure 2.

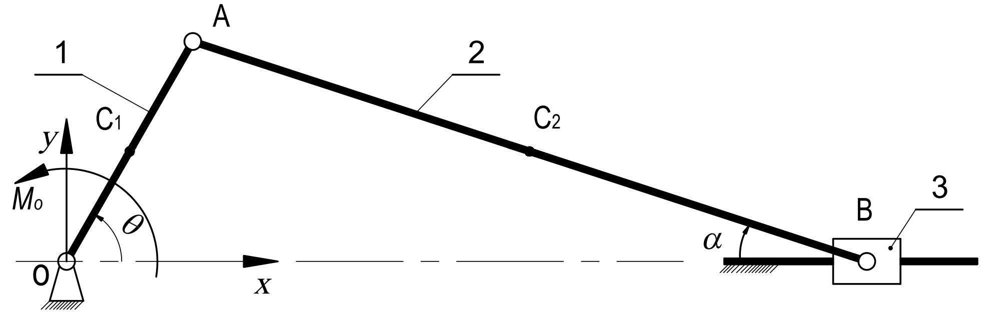

Figure 2. Slider-crank mechanism

The mechanism consists of the crank (1) characterized by length *OA=r,* mass m_1; the connecting rod (2) characterized by length *AB=l*, mass m_2; and the slider (3) characterized by m_3 and dimensionless. The motion of the mechanism is created by an active torque M_o acting at the point *O* of crank *OA*.

3.1.1. Calculating constraint force

For calculating constraint force at point *B* of the mechanism with assumption that the friction in horizontal direction is negligible, *v* is considered as the supplementary displacement. So $(q_1, q_2) = (\theta, v)$ are chosen as generalized coordinates as shown in Figure 3.

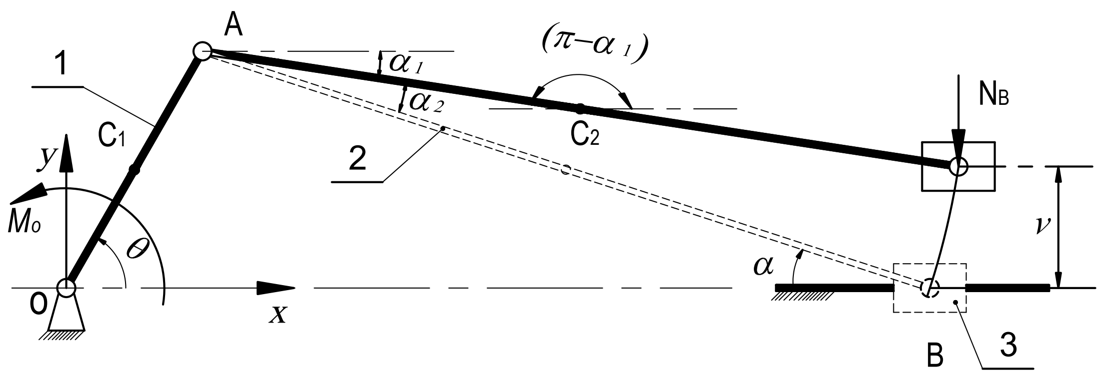

Figure 3. Virtual supplementary displacement corresponding to the constrained force

The kinetic energy has expression in the form as following

$$\begin{aligned} E = &\frac{1}{2}\{\omega_1\}^T.\{J_o\}.\{\omega_1\} + \frac{1}{2}\{\dot{r}_{C2}\}^T.m_2.\{\dot{r}_{C2}\} + \\ &+\frac{1}{2}\{\omega_2\}^T.\{J_{C2}\}.\{\omega_2\} + \frac{1}{2}\{\dot{r}_{C3}\}^T.m_3.\{\dot{r}_{C3}\} \end{aligned}, \tag{22}$$

where moments of inertia of the crank (1) with the hinged point *O*, of the connecting rod (2) with the mass center C_2 are $\{J_o\}, \{J_{C2}\}$,

$\{\omega_1\}, \{\omega_2\}$ are angular velocities measured in body reference frames,

$\{\dot{r}_{C2}\}, \{\dot{r}_{C3}\}$ are derivatives of position vectors of mass centers measured in inertial frame.

The force function producing the conservative generalized force has expression below:

$$U = -\frac{m_1 g r \sin\theta}{2} - m_2 g\left(\frac{r\sin\theta}{2} + \frac{r v^2 \sin\theta}{4(l^2 - r^2\sin^2\theta)} + \frac{v}{2}\right) - m_3 g v, \tag{23}$$

Then the conservative generalized force corresponding to v is calculated

$$Q_v^c = \frac{\partial U}{\partial v} = -\frac{m_2 g r v \sin\theta}{2\left(l^2 - r^2\sin^2\theta\right)} - \frac{m_2 g}{2} - m_3 g, \tag{24}$$

And the external generalized force acting on the mechanism corresponding to v is calculated

$$Q_v^{dib} = \frac{\delta L_v(M)}{\delta v} = 0, \tag{25}$$

After taking partial derivatives with respect to v as well as taking total derivatives for the terms relating to the Lagrange equations, and applying Eq. (21), the constraint force at the point B is

$$N_B = -\Re_v = \left[\frac{\mathrm{d}}{\mathrm{d}t}\left(\frac{\partial E}{\partial \dot{v}}\right) - \frac{\partial E}{\partial v} - \frac{\partial U}{\partial v} - \frac{\delta L_v(\vec{M})}{\delta v}\right]_{\substack{v=0\\ \dot{v}=0\\ \ddot{v}=0}}, \tag{26}$$

When the constraint force N_B is obtained, the slider-crank mechanism being as closed-loop will be transformed to open-loop by releasing the constraint at point B and putting there the constraint force as the external force acting upon the system. Thenceforth, internal forces will be determined in the open-loop in next sections.

3.1.2. Calculating axial force, shear force, and bending moment

For calculating internal forces, we need to introduce some supplementary displacement as:

- "*u*", the translation movement in direction of the center axis of the connecting rod (2), is the virtual supplementary displacement corresponding to the axial force as shown Figure 4. Thus, $(q_1, q_2) = (\theta, u)$ are chosen as generalized coordinates representing the mechanism
- "*s*", the translation movement in direction perpendicular with center axis of the connecting rod (2), is the virtual supplementary displacement corresponding to shear force as shown in Figure 5. Thus, $(q_1, q_2) = (\theta, s)$ are chosen as generalized coordinates representing the mechanism.
- "φ", the rotation movement about the axis perpendicular with vertical plane, is the virtual supplementary displacement corresponding to bending moment as shown in Figure 6. Thus, $(q_1, q_2) = (\theta, \varphi)$ are chosen as generalized coordinates representing the mechanism.

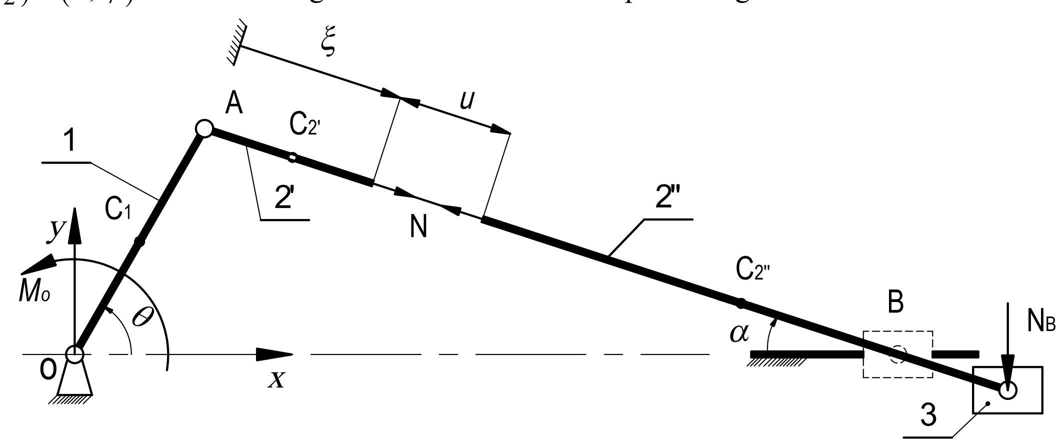

Figure 4 . Virtual supplemental displacement corresponding to the axial force

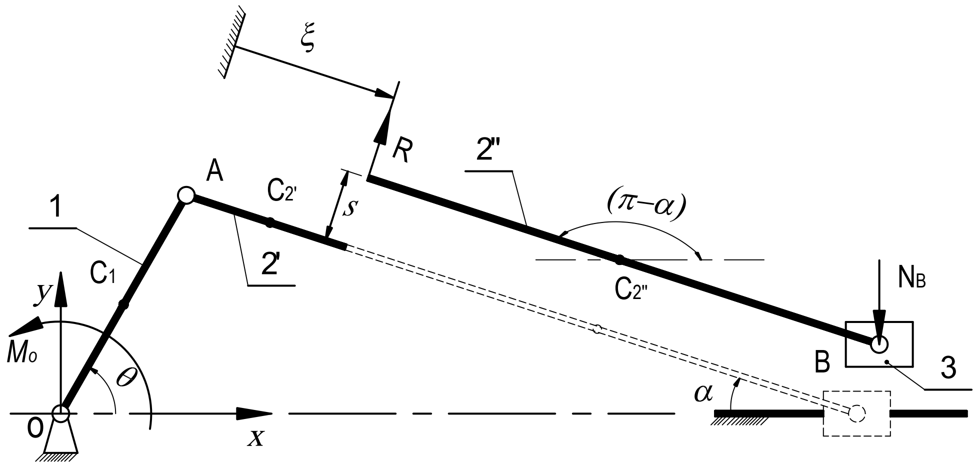

Figure 5. Virtual supplemental displacement corresponding to the shearing force

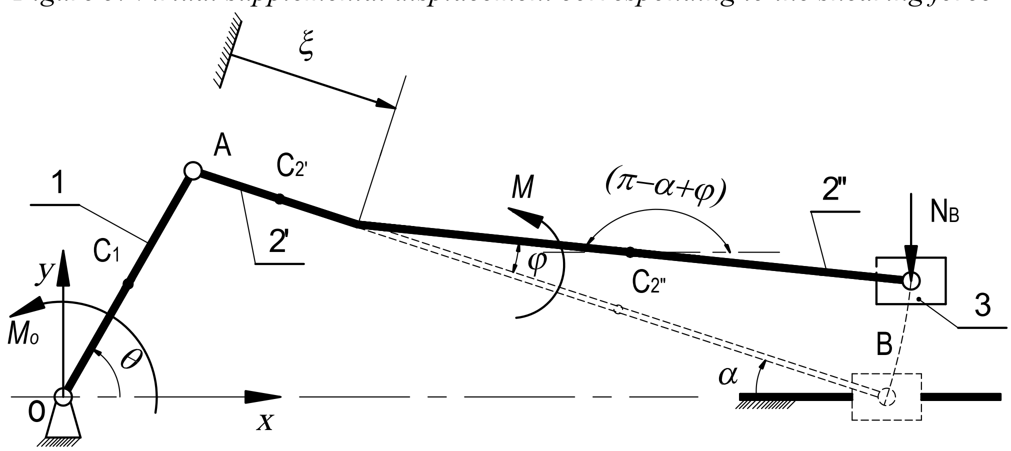

Figure 6. Virtual supplemental displacement corresponding to the bending moment

Carrying out similarly as the case for constraint force above, we will obtained the general form of internal forces by applying proposed method. Then apply law of motion for the crank (1) as:

$$\theta = \Omega_o t + \frac{\varepsilon_o}{2} t^2 , \tag{27}$$

with $\Omega_o = 25\pi \ (rad/s)$, $\varepsilon_o = \dfrac{\pi}{100} \ (rad/s^2)$

and give the slider-crank some specified dimensions, and inertia characteristics as:
$m_1 = 0.1 \ (kg)$; $r = 0.1 \ (m)$; $m_2 = 0.1 \ (kg)$; $l_2 = 0.2 \ (m)$; $m_3 = 0.1 \ (kg)$

By using Matlab software, we received graphs showing variation of constraint force with respect to time, as well as variations of internal forces with ratio ξ/l as following:

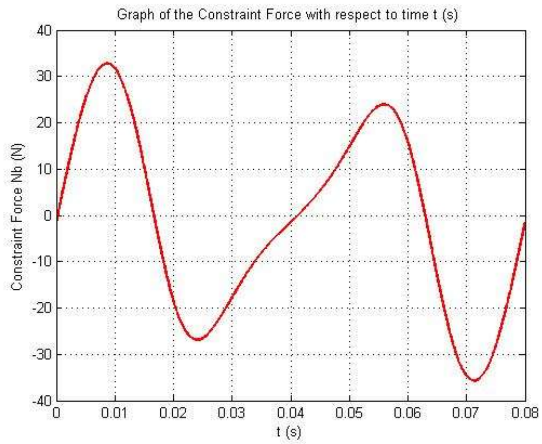

Figure 7. The constrained force at the end B with respect to time.

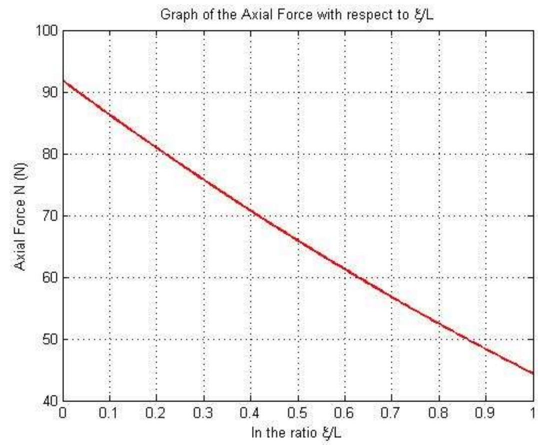

Figure 8. Variation of the axial force with respect to "ξ/l " at the instant time t=0.03(s).

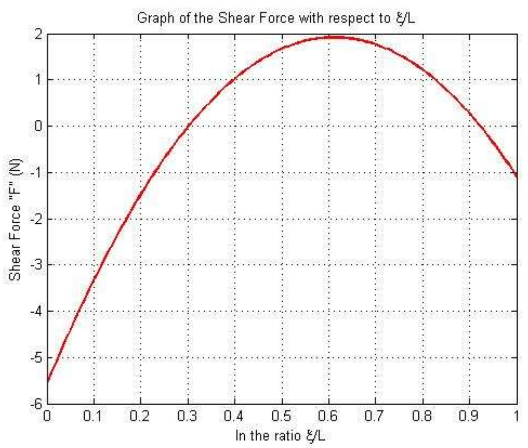

Figure 9. Variation of the shear force with respect to "ξ/l " at the instant time t=0.03(s).

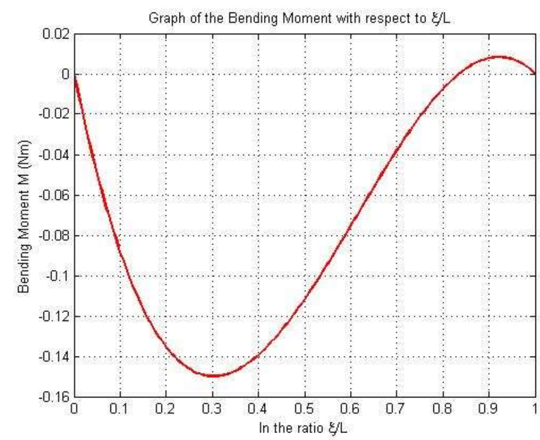

Figure 10. Variation of the bending moment w.r.t "ξ/l " at the instant time t=0.03(s).

3.2. Calculating internal forces in a group of links in mechanism

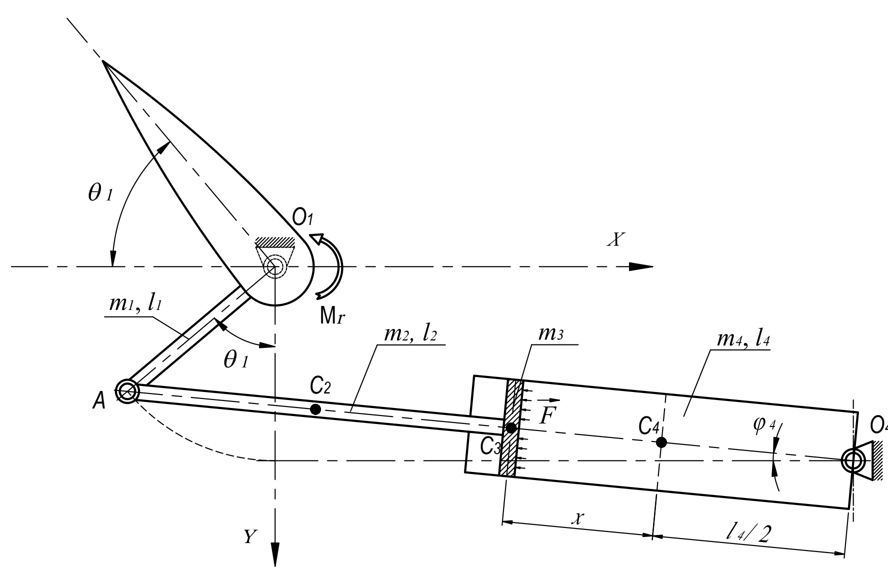

Figure 11. The system for controlling the aircraft elevator

A system for controlling the airplane elevator as shown in Figure 11 is considered as a model to calculate internal forces. For simplicity and without generality, the link (1) is supposed as a bar of length l_1 and mass m_1; the piston rod (2) is a bar characterized by the length l_2 and the mass m_2; the piston body is a plate characterized by the radius R_2 and the mass m_3; the cylinder (4) is represented by radii R_1 and R_2, the length l_4 and the mass m_4.

For more simple in finding out kinematic relations of terms related to Lagrange equations, the mechanism being closed-loop will be transferred to open-loop. For that aim, the constraint at O_4 is replaced by a constraint force acting there. And the constraint force can be considered as the sum of two components: the normal constraint force $\vec{f}_n$ with the direction along the centerline of the cylinder, and the tangent constraint force $\vec{f}_t$, with the direction perpendicular to $\vec{f}_n$. Both these two forces lie in the vertical plane.

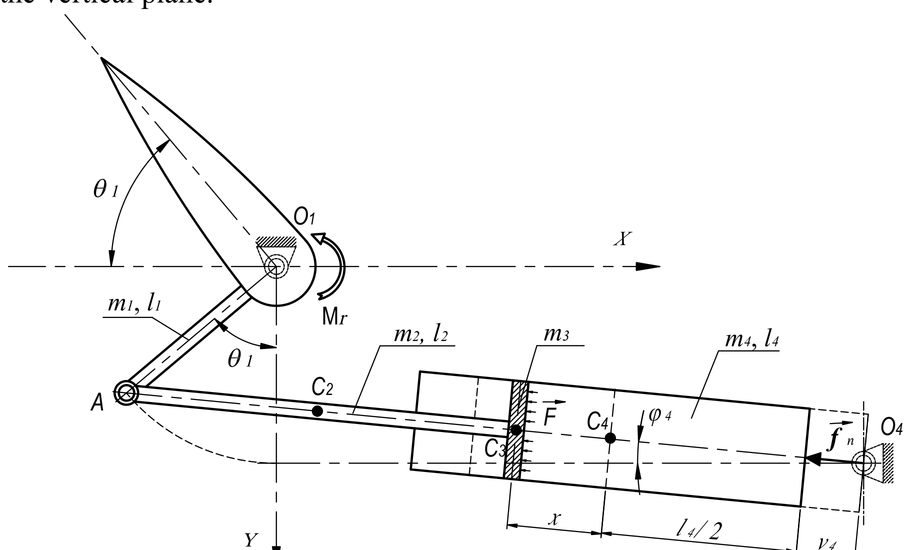

Figure 12. Diagram for calculating the normal constrained force

Supposing the supplementary mobility corresponding to the normal constraint force $\vec{f}_n$ is v_4. Thus, the generalized coordinates representing completely the considered mechanism are chosen as $(q_1, q_2) = (\theta_1, v_4)$ shown in Figure 12.

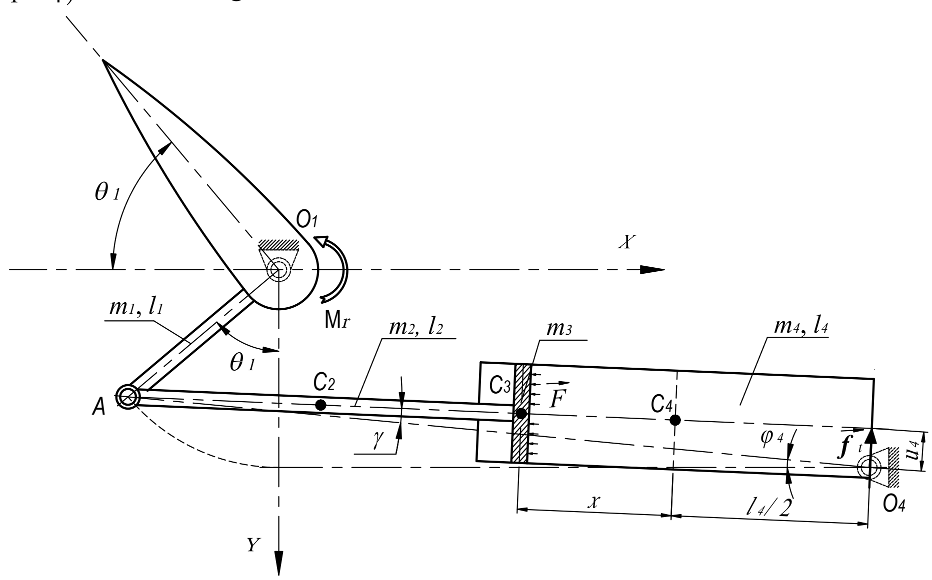

Figure 13. Diagram for calculating the tangent constrained force

Similarly, for tangent constraint force $\vec{f}_t$, the generalized coordinates are $(q_1, q_2) = (\theta_1, u_4)$ as shown in Figure 13.

And for calculating internal forces, we also introduce supplementary displacements corresponding to each case as:

- "s_1", the translation movement in direction perpendicular with center axis of the cylinder (4), is the virtual supplementary displacement corresponding to shear force as shown in Figure 14. Thus, $(q_1, q_2) = (\theta_1, s_1)$ are chosen as generalized coordinates.

- "α_3", the rotation movement about the axis perpendicular with vertical plane, is the virtual supplementary displacement corresponding to bending moment as shown in Figure 15. Thus, $(q_1, q_2) = (\theta_1, \alpha_3)$ are chosen as generalized coordinates.

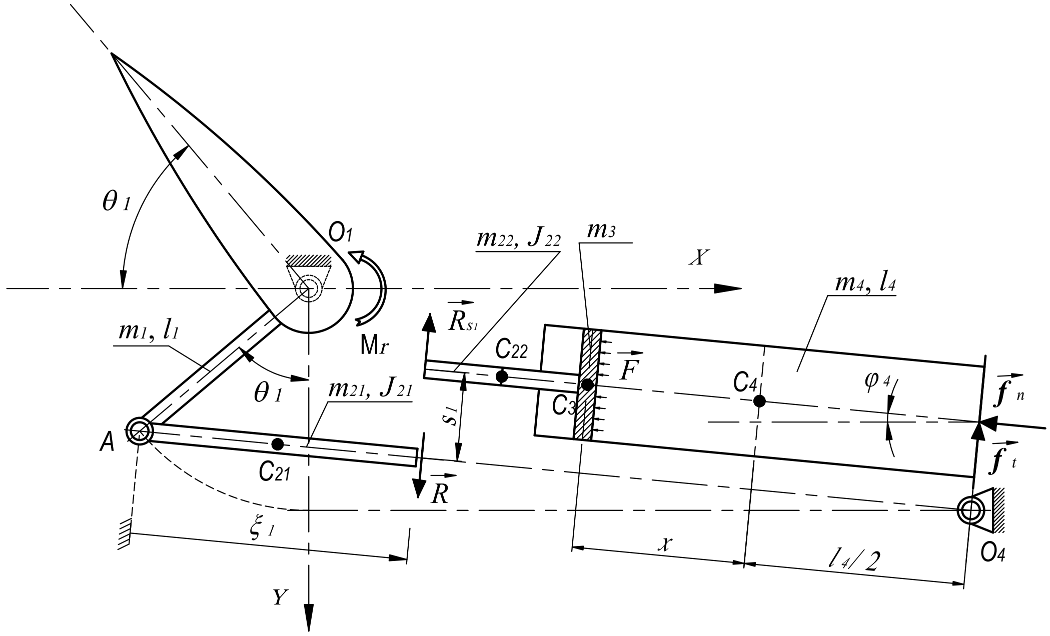

Figure 14. Diagram for calculating the shear force

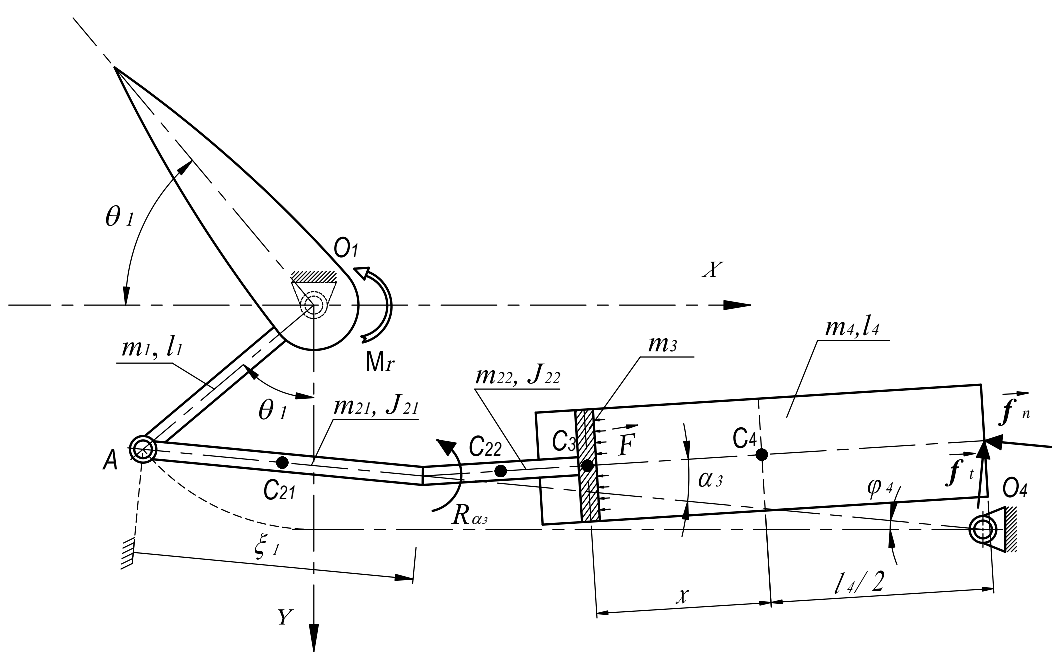

Figure 15. Diagram for calculating the bending moment

After calculating all necessary terms, then applying proposed method, internal forces will be obtained easily. And for the aim of simulation, the system for controlling the aircraft elevator is given some specified geometric and inertial characteristics as:

$l_1 = 0.5(m)$, $l_2 = 1(m)$, $l_4 = 1(m)$; $m_1 = 2(kg)$, $m_2 = 4(kg)$, $m_3 = 1(kg)$, $m_4 = 5(kg)$.

In the inverse dynamics, the link (1) is imposed by the law of motion expressed as

$$\theta_1 = \Omega_0 t + \frac{\varepsilon_0}{2} t^2, (rad), \tag{28}$$

and the moment M_r has the expression

$$M_r = \frac{9.10^4}{\pi} \theta_1, (Nm), \tag{29}$$

where $\Omega_0 = \frac{\pi}{180}, (rad/s)$; $\varepsilon_0 = \frac{\pi}{90}, (rad/s^2)$.

Based on the proposed method, the internal forces can be calculated at any position of the mechanism and at any time, corresponding to the value of the rotation angle θ_1. However, the thesis showed results for the special case when $\theta_1 = 0\ (rad)$, with the aim to compare them with the results calculated for the static system mentioned below. By using Matlab software, the bending moment *M_{bd}*, and the shear force *F_1* with respect to " $\frac{\xi_1}{\left(l_2 + {}^{l_4}\!/_2 + x\right)}$ " along the length of piston rod-cylinder subsystem are released as shown in Figure 16 and Figure 17, respectively.

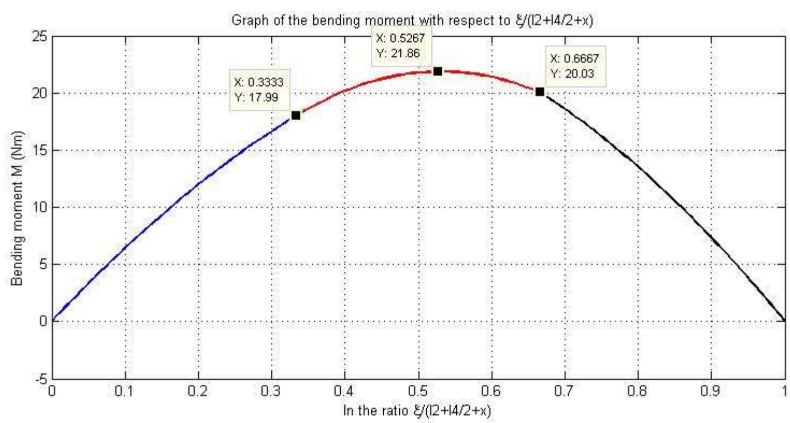

Figure 16. Variation of the bending moment along the piston rod-cylinder at $\theta_1 = 0$ (rad)

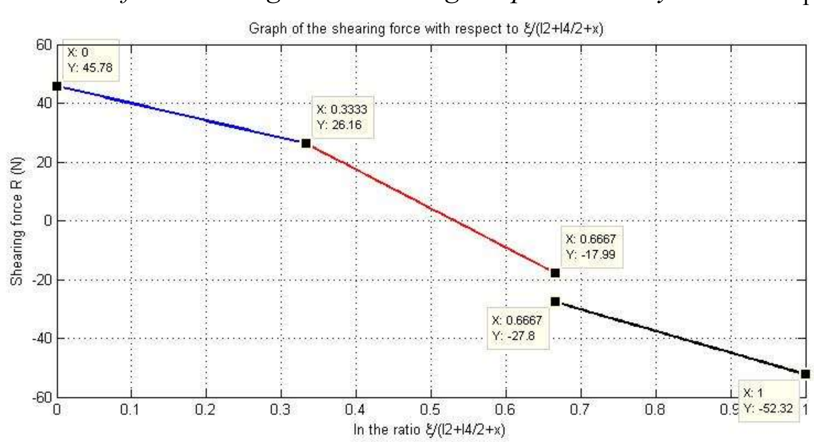

Figure 17. Variation of the shear force along the piston rod-cylinder at $\theta_1 = 0$ (rad)

In order to verify the results above, the system for controlling the aircraft elevator at the position $\theta_1 = 0\,(rad)$ is simplified as a static system, which is considered a beam acted by distributed and concentrated forces, which are compatible with the given geometric and inertia characteristics of the mechanism. Then, by using the section method to compute manually the shear force and the bending moment, the results shown in Figure 18 were obtained.

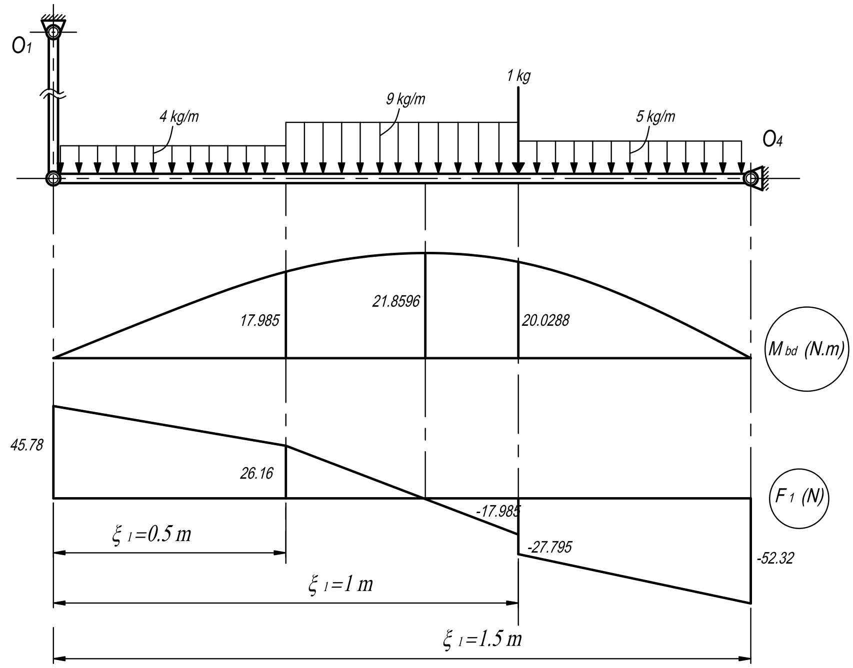

Figure 18. The internal force diagram of the simplified model

4. Calculus of internal forces in spatial mechanisms

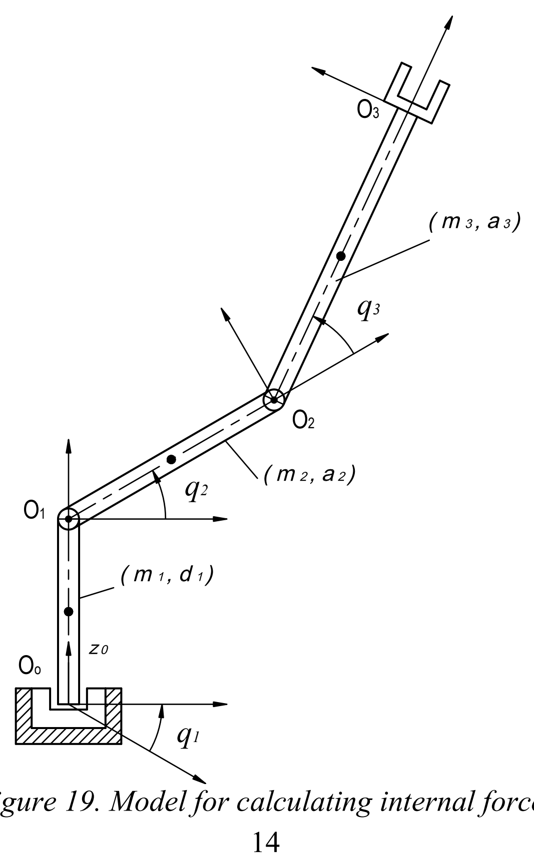

Figure 19. Model for calculating internal forces

The spatial serial manipulator as shown in Figure 19 is considered as model for calculating internal forces. The mechanism is one kind of the most popular manipulators having three degrees of freedom corresponding to three independent angular variables q_1, q_2 and q_3.

For determining internal forces in end-effector of the mechanism mentioned above by using Lagrange equations, kinematic relations of links in the mechanism must be calculated first, in particular here is linear and angular velocities. For a long time, Denavit-Hatenberg Convention is well-known approach for analyzing kinematic relations between links in robotic field. Besides, this section will use also a direct way presented previously to determine kinematic relations of links based on positions and orientations of links' body reference frame. Then results determined in two cases are compared each other to verify validity of proposed measure.

4.1. Calculus of axial force in the end-effector

For calculating axial force in the rod of end-effector, we must assign coordinates systems for links of the mechanism. Once origins and coordinates systems are assigned completely, we can choose the independent variables describing the mechanism's configuration in the most appropriate manner. And they are specified and shown more detail in the figures below corresponding to the case of analyzing kinematic relations directly or by using Denavit-Hatenberg Convention.

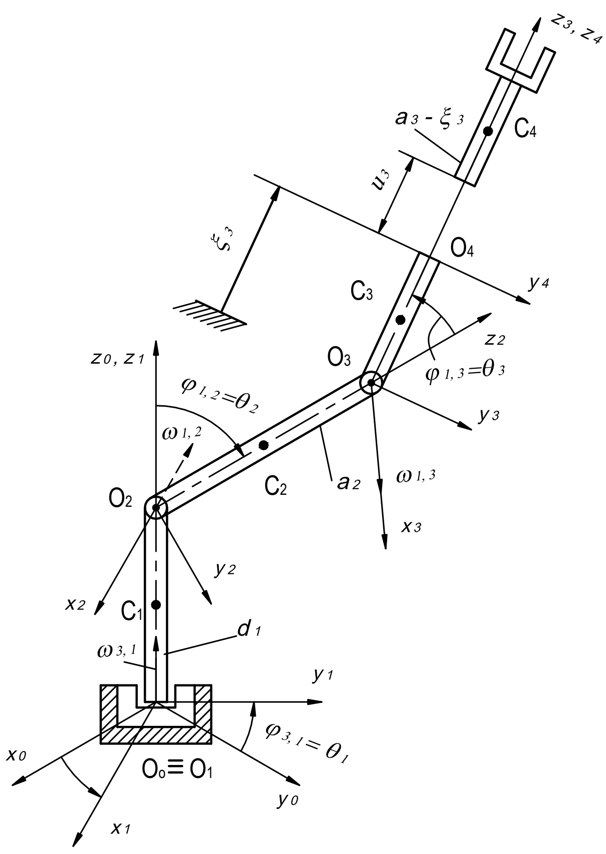

Figure 20. Assigning coordinates diagram for calculating axial force directly

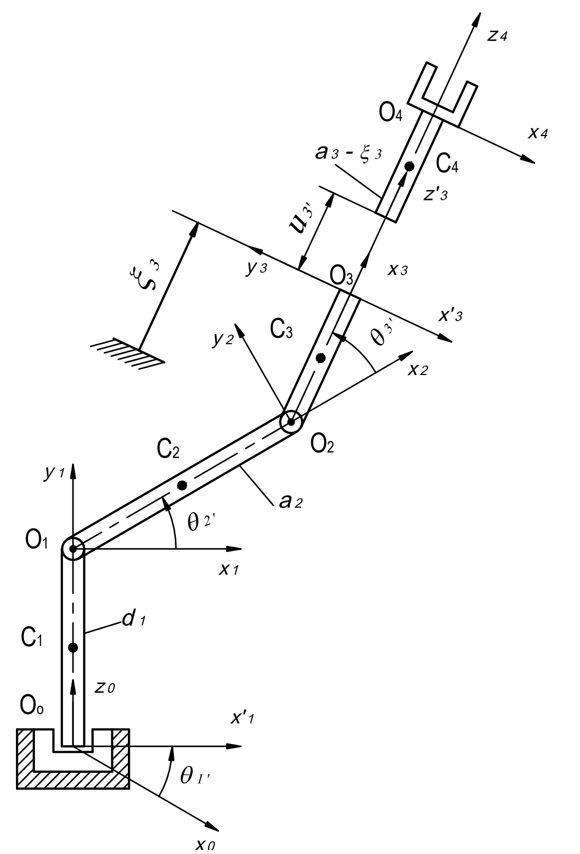

Figure 21. Assigning coordinates diagram for calculating axial fore with Denavit-Hatenberg

For case analyzing kinematic relations directly, the generalized coordinates representing completely for the mechanism are chosen as $q=(q_1,q_2,q_3,q_4)\equiv(\theta_1,\theta_2,\theta_3,u_3)$ shown in Figure 20.

For using Denavit-Hatenberg Convention, the generalized coordinates representing completely for the mechanism are chosen as $q=(q_1,q_2,q_3,q_4)\equiv(\theta_{1'},\theta_{2'},\theta_{3'},u_{3'})$ shown in Figure 21.

After computing terms relating to the Lagrange equations, then applying Eq. (21), the axial force in the end-effector is achieved corresponding to each case:

$$N_3 = \left[\frac{\mathrm{d}}{\mathrm{d}t}\left(\frac{\partial E}{\partial \dot{u}_3}\right) - \frac{\partial E}{\partial u_3} - \frac{\partial U}{\partial u_3}\right]_{\substack{u_3=0\\ \dot{u}_3=0\\ \ddot{u}_3=0}}$$

$$= \frac{-m_3\left(a_3-\xi_3\right)}{4a_3}.\begin{pmatrix} 4a_2.\ddot{\theta}_2.\sin\theta_3 - 4(a_3+\xi_3).\dot{\theta}_2.\dot{\theta}_3 + \\ +\begin{pmatrix} a_3+\xi_3-\xi_3.\cos(2\theta_2-2\theta_3)+2a_2.\cos\theta_3 + \\ -2a_2\cos(2\theta_2-\theta_3)-a_3.\cos(2\theta_2-2\theta_3)\end{pmatrix}.\dot{\theta}_1^2 + \\ +(2a_3+2\xi_3+4a_2.\cos\theta_3).\dot{\theta}_2^2 + \\ +(2a_3+2\xi_3).\dot{\theta}_3^2 - 4g.\cos(\theta_2-\theta_3) \end{pmatrix} \tag{30}$$

$$N_{3'} = \left[\frac{\mathrm{d}}{\mathrm{d}t}\left(\frac{\partial E}{\partial \dot{u}_{3'}}\right) - \frac{\partial E}{\partial u_{3'}} - \frac{\partial U}{\partial u_{3'}}\right]_{\substack{u_{3'}=0\\ \dot{u}_{3'}=0\\ \ddot{u}_{3'}=0}}$$

$$= \frac{-m_3\left(a_3-\xi_3\right)}{4a_3}.\begin{pmatrix} -4a_2.\ddot{\theta}_{2'}.\sin\theta_{3'} + 4(a_3+\xi_3).\dot{\theta}_{2'}.\dot{\theta}_{3'} + \\ +\begin{pmatrix} a_3+\xi_3+\xi_3.\cos(2\theta_{2'}+2\theta_{3'})+2a_2.\cos\theta_{3'} + \\ +2a_2\cos(2\theta_{2'}+\theta_{3'})+a_3.\cos(2\theta_{2'}+2\theta_{3'})\end{pmatrix}.\dot{\theta}_{1'}^2 + \\ +(2a_3+2\xi_3+4a_2.\cos\theta_{3'}).\dot{\theta}_{2'}^2 + \\ +(2a_3+2\xi_3).\dot{\theta}_{3'}^2 - 4g.\sin(\theta_{2'}+\theta_{3'}) \end{pmatrix}, \tag{31}$$

4.2. Calculus of shear force in the end-effector

Similarly, for calculating shear force in the rod of end-effector, assignment of coordinates systems for links of the mechanism are performed thoughtfully. Then choosing generalized coordinates the most compatibly with the case of analyzing kinematic relations directly or by using Denavit-Hatenberg Convention is shown in figures below.

For case analyzing kinematic relations directly, the generalized coordinates are chosen as $q=\left(q_1,q_2,q_3,q_4\right)\equiv\left(\theta_1,\theta_2,\theta_3,S_3\right)$ shown in Figure 22.

For using Denavit-Hatenberg Convention, the generalized coordinates are chosen as $q=\left(q_1,q_2,q_3,q_4\right)\equiv\left(\theta_{1'},\theta_{2'},\theta_{3'},S_{3'}\right)$ shown in Figure 23.

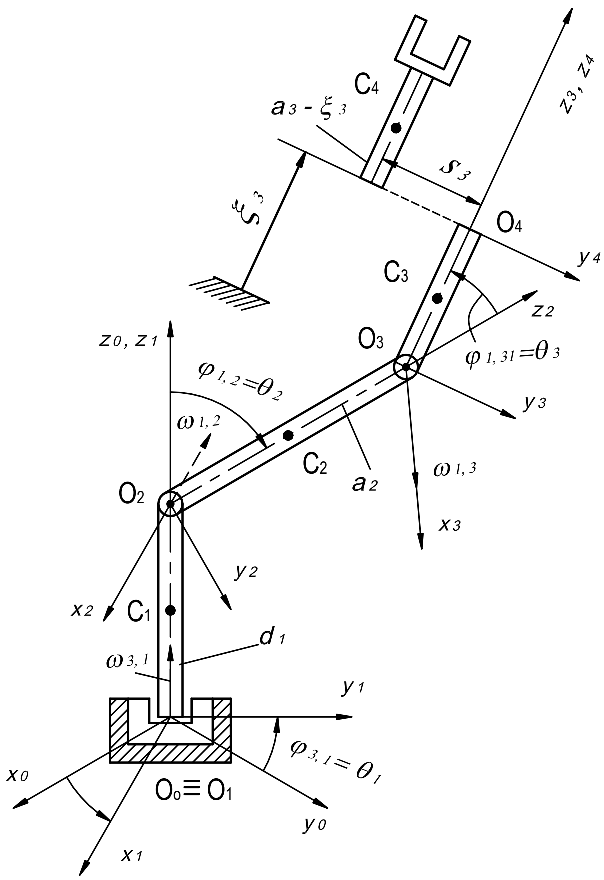

Figure 22. Assigning coordinates diagram for calculating shear force directly

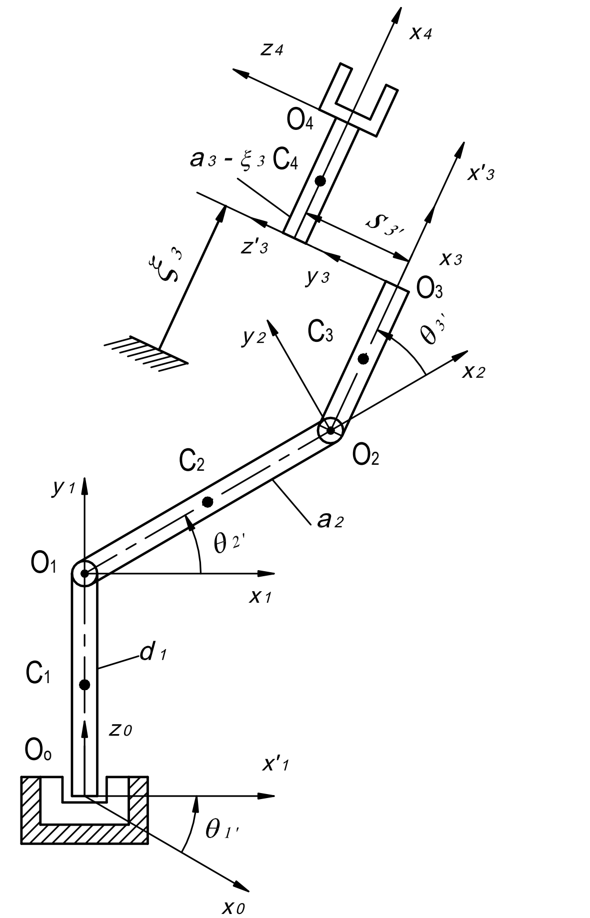

Figure 23. Assigning coordinates diagram for calculating shear fore with Denavit-Hatenberg

After computing terms relating to the Lagrange equations, then applying Eq. (21), the shear force in the end-effector is achieved corresponding to each case:

$$F_3 = \left[\frac{\mathrm{d}}{\mathrm{d}t}\left(\frac{\partial E}{\partial \dot{s}_3}\right) - \frac{\partial E}{\partial s_3} - \frac{\partial U}{\partial s_3} \right]_{\substack{s_3=0 \\ \dot{s}_3=0 \\ \ddot{s}_3=0}}$$

$$= \frac{m_3(a_3-\xi_3)}{4a_3} \cdot \begin{pmatrix} (2a_3+2\xi_3).\ddot{\theta}_3 - (2a_3+2\xi_3+4a_2.\cos\theta_3).\ddot{\theta}_2 + \\ + \begin{pmatrix} 2a_2.\sin(2\theta_2-\theta_3) + a_3.\sin(2\theta_2-2\theta_3) + \\ +\xi_3.\sin(2\theta_2-2\theta_3) + 2a_2.\sin\theta_3 \end{pmatrix} .\dot{\theta}_1^2 + \\ +4a_2.\dot{\theta}_2^2.\sin\theta_3 + 4g.\sin(\theta_2-\theta_3) \end{pmatrix}, \tag{32}$$

$$F_{3'} = \left[\frac{\mathrm{d}}{\mathrm{d}t}\left(\frac{\partial E}{\partial \dot{s}_{3'}}\right) - \frac{\partial E}{\partial s_{3'}} - \frac{\partial U}{\partial s_{3'}}\right]\Bigg|_{\substack{s_{3'}=0\\ \dot{s}_{3'}=0\\ \ddot{s}_{3'}=0}}$$

$$= \frac{m_3\left(a_3-\xi_3\right)}{4a_3}.\left(\begin{array}{l} \left(2a_3+2\xi_3\right).\ddot{\theta}_{3'} + \left(2a_3+2\xi_3+4a_2.\cos\theta_{3'}\right).\ddot{\theta}_{2'} + \\ +\left(\begin{array}{l} 2a_2.\sin(2\theta_{2'}+\theta_{3'}) + a_3.\sin(2\theta_{2'}+2\theta_{3'}) + \\ +\xi_3.\sin(2\theta_{2'}+2\theta_{3'}) + 2a_2.\sin\theta_{3'} \end{array}\right).\dot{\theta}_{1'}^2 + \\ +4a_2.\dot{\theta}_{2'}^2.\sin\theta_{3'} + 4g.\sin(\theta_{2'}+\theta_{3'}) \end{array}\right), \tag{33}$$

4.3. Calculus of bending moment in the end-effector

For case analyzing kinematic relations directly, the generalized coordinates are chosen as $q=\left(q_1,q_2,q_3,q_4\right)\equiv\left(\theta_1,\theta_2,\theta_3,\varphi_3\right)$ shown in Figure 24.

For using Denavit-Hatenberg Convention, the generalized coordinates are chosen as $q=\left(q_1,q_2,q_3,q_4\right)\equiv\left(\theta_{1'},\theta_{2'},\theta_{3'},\varphi_{3'}\right)$ shown in Figure 25.

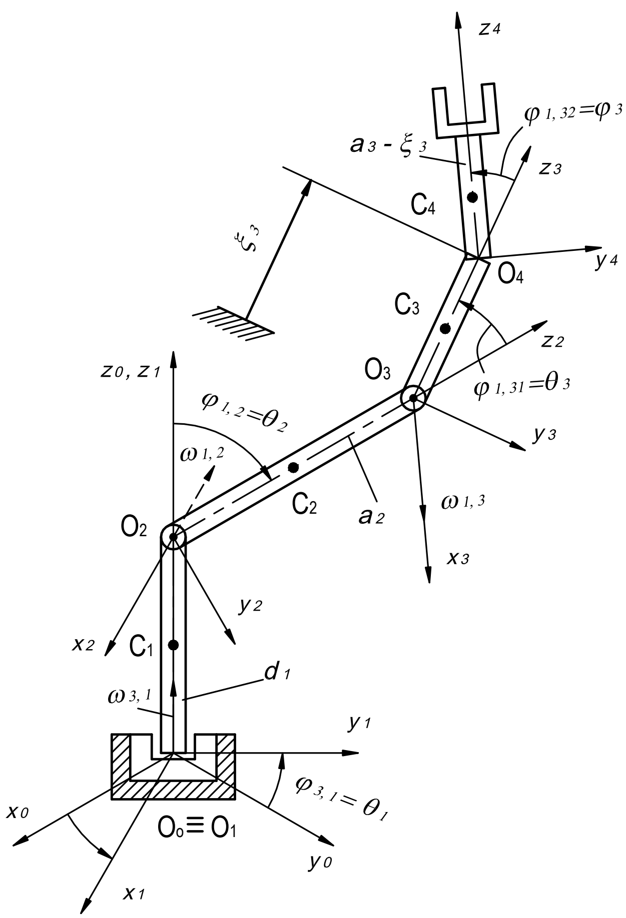

Figure 24. Assigning coordinates diagram for calculating bending moment directly

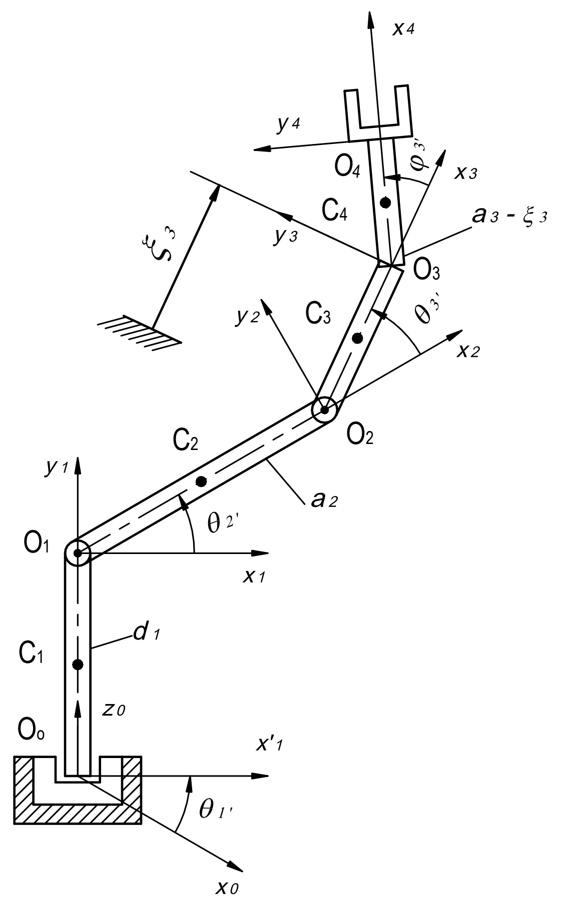

Figure 25. Assigning coordinates diagram for calculating bending moment with D-H

After computing terms relating to the Lagrange equations, then applying Eq. (21), the bending moment in the end-effector is achieved corresponding to each case:

$$M_3 = -\left[\frac{\mathrm{d}}{\mathrm{d}t}\left(\frac{\partial E}{\partial \dot{\varphi}_3}\right) - \frac{\partial E}{\partial \varphi_3} - \frac{\partial U}{\partial \varphi_3}\right]\Bigg|_{\substack{\varphi_3 = 0\\ \dot{\varphi}_3 = 0\\ \ddot{\varphi}_3 = 0}}$$

$$= \frac{-m_3\left(a_3 - \xi_3\right)^2}{12a_3} \cdot \begin{pmatrix} (4a_3 + 2\xi_3).\ddot{\theta}_3 - (4a_3 + 2\xi_3 + 6a_2.\cos\theta_3).\ddot{\theta}_2 + \\ + \begin{pmatrix} 3a_2.\sin(2\theta_2 - \theta_3) + 2a_3.\sin(2\theta_2 - 2\theta_3) + \\ + \xi_3.\sin(2\theta_2 - 2\theta_3) + 3a_2.\sin\theta_3 \end{pmatrix}.\dot{\theta}_1^2 + \\ + 6a_2.\dot{\theta}_2^2.\sin\theta_3 + 6g.\sin(\theta_2 - \theta_3) \end{pmatrix}, \quad (34)$$

$$M_{3'} = -\left[\frac{\mathrm{d}}{\mathrm{d}t}\left(\frac{\partial E}{\partial \dot{\varphi}_{3'}}\right) - \frac{\partial E}{\partial \varphi_{3'}} - \frac{\partial U}{\partial \varphi_{3'}}\right]\Bigg|_{\substack{\varphi_{3'} = 0\\ \dot{\varphi}_{3'} = 0\\ \ddot{\varphi}_{3'} = 0}}$$

$$= \frac{-m_3\left(a_3 - \xi_3\right)^2}{12a_3} \cdot \begin{pmatrix} (4a_3 + 2\xi_3).\ddot{\theta}_{3'} + (4a_3 + 2\xi_3 + 6a_2.\cos\theta_{3'}).\ddot{\theta}_{2'} + \\ + \begin{pmatrix} 3a_2.\sin(2\theta_{2'} + \theta_{3'}) + 2a_3.\sin(2\theta_{2'} + 2\theta_{3'}) + \\ + \xi_3.\sin(2\theta_{2'} + 2\theta_{3'}) + 3a_2.\sin\theta_{3'} \end{pmatrix}.\dot{\theta}_{1'}^2 + \\ + 6a_2.\dot{\theta}_{2'}^2.\sin\theta_{3'} + 6g.\cos(\theta_{2'} + \theta_{3'}) \end{pmatrix}, \quad (35)$$

5. Controlling motion of a spatial 4-DOF manipulator

5.1. Simulating model and equations of motion

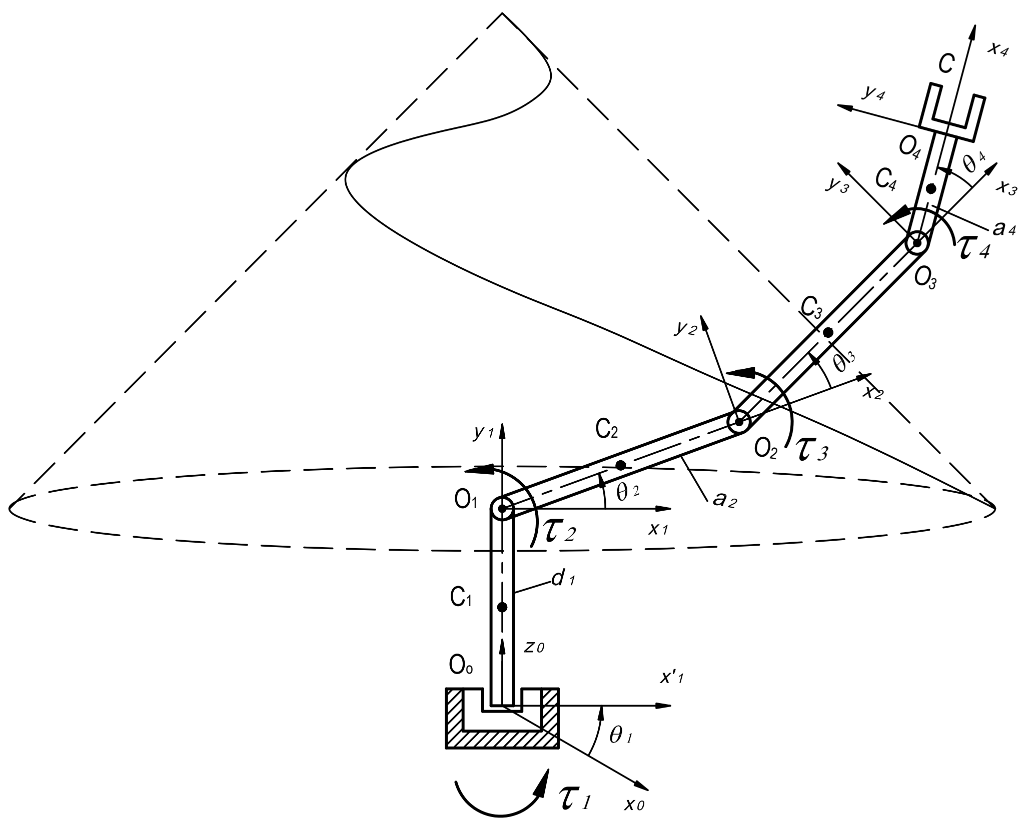

Figure 26. The 4-DOF manipulator

For our purpose of giving control law of a mechanism, let's consider the 4-DOF articulated manipulator as shown in Figure 26. The first link (1) characterized by length d_1 and mass m_1 is subjected to the external torque τ_1, which has its effect in horizontal plane, at the point O_0. Analogously, the links (2), (3) and (4) characterized by lengths a_2, a_3, a_4 and masses m_2, m_3, m_4, are actuated by the external torques τ_2, τ_3, τ_4, which have their effects in vertical plane, at the points O_1, O_2, O_3, respectively.

As shown, the manipulator has four degrees of freedom, thus let's choose angle vector $\theta = [\theta_1, \theta_2, \theta_3, \theta_4]$, in which the angles are assigned according to DH Convention, as the generalized coordinates. Then the equations of motion are written easily using Lagrange equation:

$$\frac{\mathrm{d}}{\mathrm{d}t}\left(\frac{\partial E}{\partial \dot{\theta}_i}\right) - \frac{\partial E}{\partial \theta_i} = Q_i^* + \frac{\partial U}{\partial \theta_i}, \quad (i = 1, 2, 3, 4), \tag{36}$$

where E is the total kinetic energy of mechanism,

U is the force function,

Q_i^* is the external generalized force acting on the link *i*, in this case $Q_i^* = \tau_i, \ (i = 1,2,3,4)$.

From geometric and kinematic relationship between the links of the manipulator, after computing all necessary terms then replacing them into Eq. (36), the equations of motion are obtained in matrix form as following:

$$\mathbf{A}\ddot{\boldsymbol{\theta}} - \mathbf{B} = \boldsymbol{\tau}, \tag{37}$$

where $\ddot{\boldsymbol{\theta}} = \left[\ddot{\theta}_1, \ddot{\theta}_2, \ddot{\theta}_3, \ddot{\theta}_4\right]^T$ is the vector of second time derivative of the joint coordinates,

$\boldsymbol{\tau} = [\tau_1, \tau_2, \tau_3, \tau_4]^T$ is the external torque vector acting on the links at the points O_0, O_1, O_2, and O_3, respectively,

$$\mathbf{A} = \begin{bmatrix} a_{11} & a_{12} & a_{13} & a_{14} \\ a_{21} & a_{22} & a_{23} & a_{24} \\ a_{31} & a_{32} & a_{33} & a_{34} \\ a_{41} & a_{42} & a_{43} & a_{44} \end{bmatrix}$$ is the inertia matrix.

5.2. Determining optimal parameters of PID controllers by using the GA

Let's consider one simple example: Control the tip of end-effector of the 4-DOF manipulator above to follow the specified trajectory on surface of cone in the plane *Oxyz* written in the function as following:

$$\sqrt{x^2 + y^2} + z = 0.25 \ (m), \tag{38}$$

Or it can be written in form with respect to time as:

$$\begin{cases} r = \sqrt{x^2 + y^2} = 0.25\left(1 - \dfrac{t - t_o}{T_f - t_o}\right) = 0,25.\left(1 - \dfrac{t}{20}\right) \ (m) \\ z = 0.25\dfrac{t - t_o}{T_f - t_o} = 0,25.\dfrac{t}{20} \ (m) \end{cases}, \tag{39}$$

in there, *r* represents the radius,

z represents the height,

$t_o = 0, \ T_f = 20\,(s)$ are the initial and final times of the analysis process.

There are many methods to control the 4-DOF manipulator, but in this case we use PID controllers to control the manipulator thanks to their simplicity and transparence. As known, one of the most common difficulties when using the PID controllers is to determine the optimal parameters, i.e: the proportional gain K_P, the integral gain K_I, and the derivative gain K_D

because of the constantly changing of the system parameters in almost all processes. To overcome that tough issue, a GA is used for finding out parameters of PID controllers. The block diagram of our control system using the GA for determining the optimal PID parameters is shown in Figure 27.

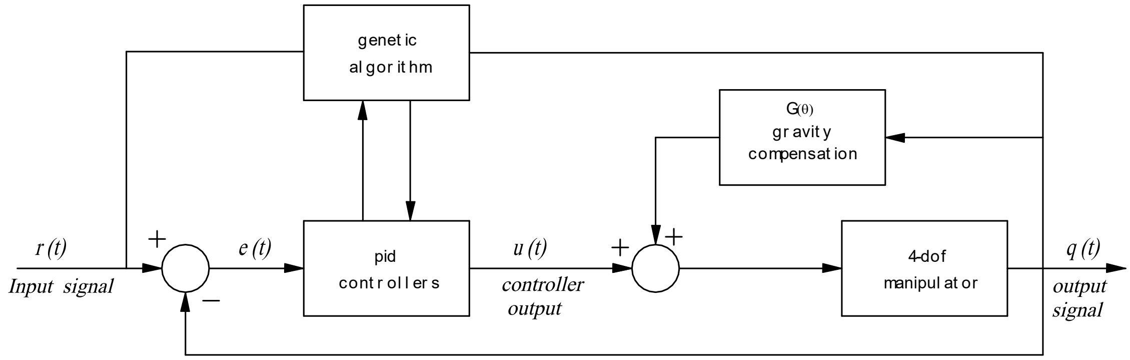

Figure 27. PID tuning diagram with the GA

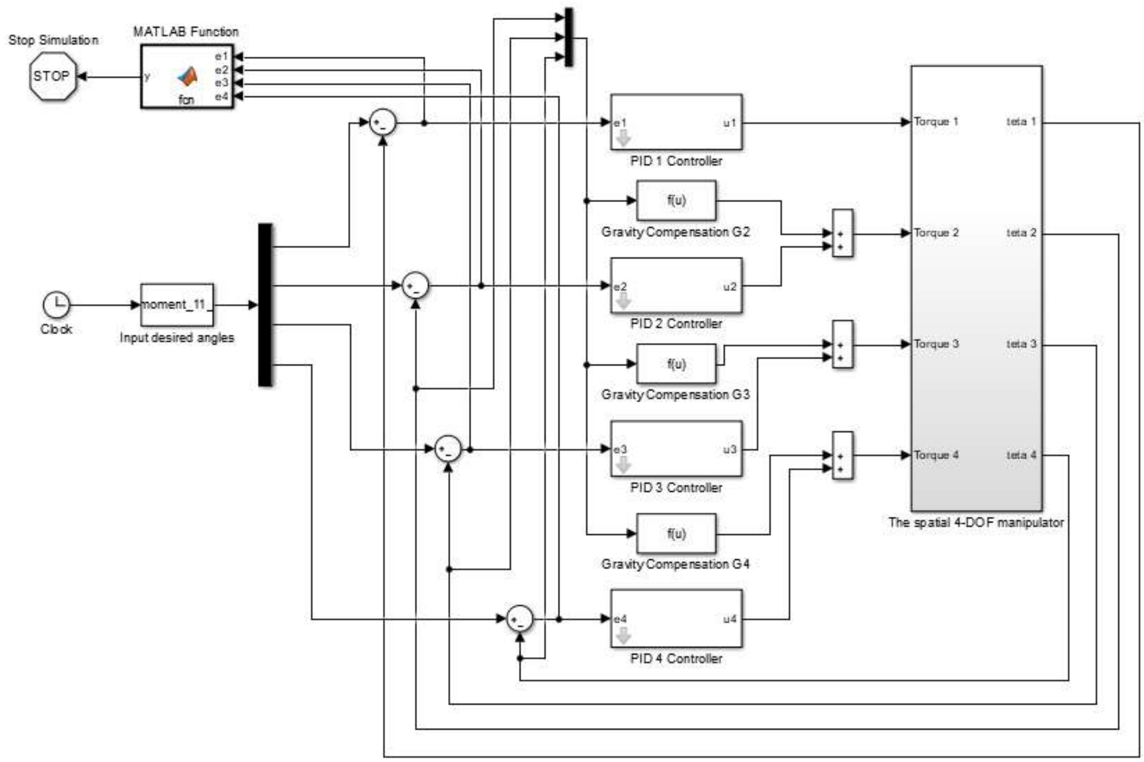

Figure 28. Completed scheme of 4-DOF manipulator with PID controllers

For the simulation purpose, let's consider that the 4-DOF manipulator has the following inertial and geometric data: $m_1 = m_2 = m_3 = m_4 = 0.1(kg)$; $d_1 = 0.1(m)$; $a_2 = a_3 = 0.13(m)$; $a_4 = 0.04\ (m)$ and that the initial state of the manipulator considered in the case study is

$$\theta_1(t_o) = 0\ (rad), \qquad \dot{\theta}_1(t_o) = 0.03927\ (rad/s),$$

$$\theta_2(t_o) = -0.663070\ (rad), \qquad \dot{\theta}_2(t_o) = -0.056864\ (rad/s),$$

$$\theta_3(t_o) = 1.072371\ (rad), \qquad \dot{\theta}_3(t_o) = 0.210525\ (rad/s),$$

$$\theta_4(t_o) = 0.376097\ (rad), \qquad \dot{\theta}_4(t_o) = -0.153661\ (rad/s).$$

Using Mathlab software, and after applying GA for tuning PID controllers in our system, the values of K_{Pi}, K_{Ii}, K_{Di} (i=1, 2, 3, 4) are determined as:

$K_{P1} = 26.7600$; $K_{I1} = 1.1200$; $K_{D1} = -0.2500$;

$K_{P2} = 19.4350$; $K_{I2} = 21.2450$; $K_{D2} = -0.7900$;

$K_{P3} = 0.8100$; $K_{I3} = 0.1950$; $K_{D3} = -0.2850$;

$K_{P4} = 0.0160$; $K_{I4} = 0.0070$; $K_{D4} = -0.0020$.

The results obtained from Simulink model (and also SimMechanics model) corresponding to the above value of PID parameters are shown below.

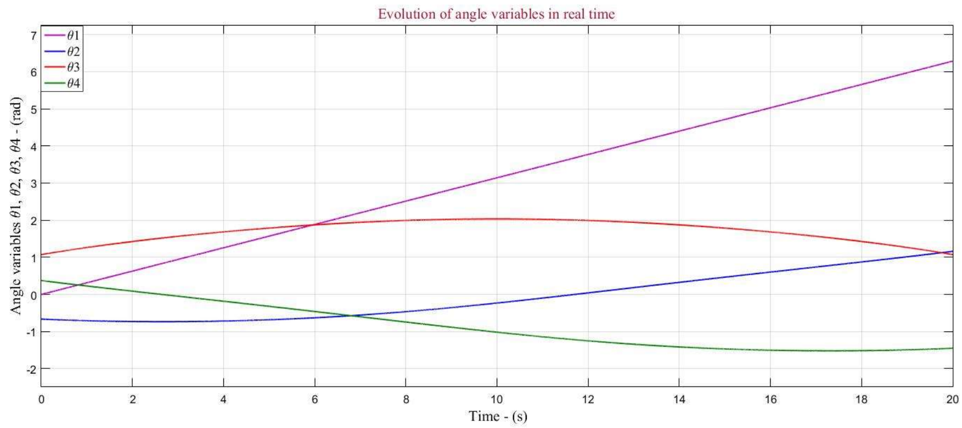

Figure 29. Evolution of the joint coordinates θ_1, θ_2, θ_3, θ_4 versus real time

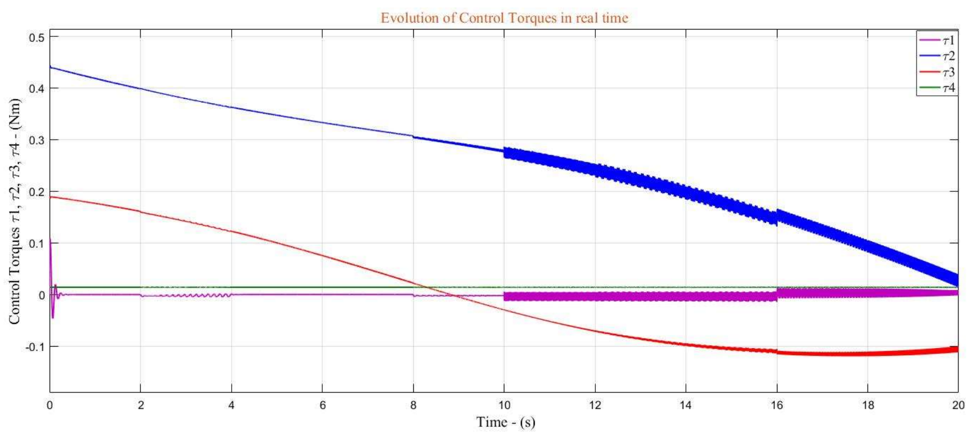

Figure 30. Evolution of the external torques τ_1, τ_2, τ_3, τ_4 versus real time

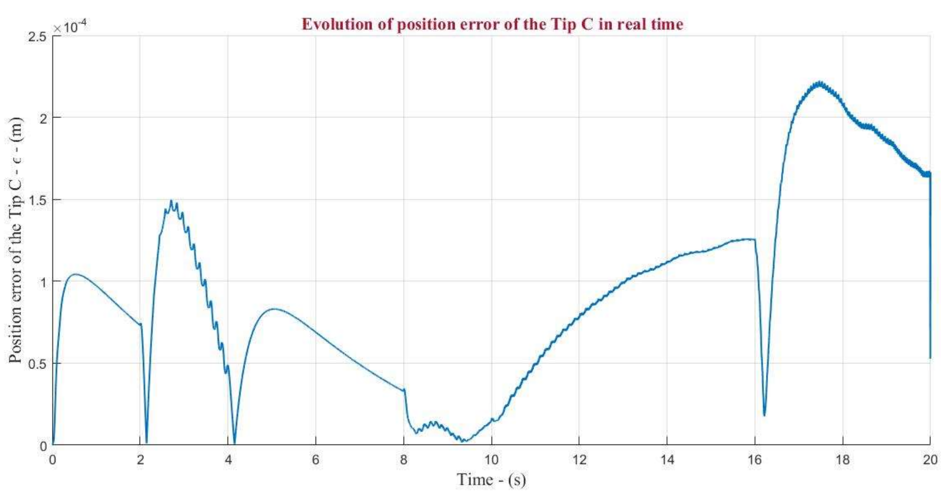

Figure 31. Position error of the end-effector in real time

With the aim of illustrating how well the manipulator performed the given task with computed value of PID parameters, the position error showing the difference between real position of the end-effector and its desirable position is considered, and is defined by:

$$\varepsilon_C(t)=\sqrt{\left(\sqrt{x_C^{real}(t)^2+y_C^{real}(t)^2}-\sqrt{x_C^{des}(t)^2+y_C^{des}(t)^2}\right)^2+\left(z_C^{real}(t)-z_C^{des}(t)\right)^2}\ , \tag{40}$$

where $\varepsilon_C(t)$ is square root of square position error,

$x_C^{real}(t),\ y_C^{real}(t),\ z_C^{real}(t)$ are real coordinates of the end-effector on axes with respect to time,

$x_C^{des}(t),\ y_C^{des}(t),\ z_C^{des}(t)$ are desirable coordinates of the end-effector on axes with respect to time.

As shown in Figure 31, the position error of the end-effector remains in the range of [0; 0.25 mm]. In practice, this error is due to accumulation errors and is acceptable, taking into account the length of trajectory of the 4-DOF serial manipulator. This error can be reduced by improving the GA program to give the better solutions of the PID parameters.

6. Conclusions and Future Works

Based on the fundamental definitions of rigid body mechanics, this thesis presented a new method derived from Lagrange equations to calculate internal forces in an arbitrary link in a rigid body system. This work is really significant, especially for a complex rigid body system possessing many links due to without considering constraint forces in calculating process. From the proposed method, the thesis calculated internal forces in closed mechanism as well as in open one. Besides, the thesis also applied Genetic Algorithms in tuning parameters of PID controllers to control a 4-DOF mechanism to perform a given task.

The models used in this thesis ignored friction force, damping force… during calculating process, so we can take into account the effect of friction in the contact surfaces between links, as well as effect of damping force in hydraulic cylinder in order to make it close to practice.

Modeling and simulating the mechanism on dynamic software such as ADAMS with the identical conditions applied, then calculating the load and stress distributed throughout the mechanism. Based on that, we compare with the results obtained by proposed method.

Considering the mechanism again, we apply the proposed method to compute internal forces. Then comparing results obtained in two ways.

For controlling model, we can improve the genetic algorithm in order to tune the PID parameters faster and to get better control quality, i.e the position error of the tip of end-effector is reduced and smaller than the result achieved above.

SELECTIVE BIBLIOGRAPHY

[1] Ahmed A. Shabana, *Dynamics of Multibody Systems*, Cambridge University Press, Third Edition, 374 pages, 2005.

[2] Lenarcic, Jadran, Bajd, Tadej, Stanišić**,** Michael M, *Robot Mechanism,* International Series on Intelligent Systems, Control, and Automation: Science and Engineering, Springer, 347 pages, 2012.

[3] I. Stroe, S. Staicu, *Calculus of joint forces using Lagrange equations and principle of virtual work*, Proceedings of the Romanian Academy, Series A, Volume 11, pp. 253-260, 2010.

[4] I. Stroe, *Kinetics of Multibody Systems in Gravity Field*, The Eight IFToMM International Symposium on Theory of Machines and Mechanisms, Bucharest-Romania, Vol. II, pp. 309-314, August 28-September 1, 2001.

[5] I. Stroe, *Multibody Systems with Holonomic and Nonholonomic Constraints, Virtual Nonlinear Mutibody Systems*, NATO Advanced Study Institute, Vol. I, Edited by Werner Schiehlen and Michael Valasek, Prague, pp. 183-189, June 23-July 3, 2002.

[6] I. Stroe, M.I. Piso, S. Zaharia, G.V. Manciu, *Multibody Systems in Central Gravitational Field*, IC-SCCE, International Conference "From Scientific Computing to Computational Engineering" , Athens, Greece, July, 2006.

[7] I. Stroe, P. Parvu, D. Caruntu, *Multibody Systems with Holonomic and Nonholonomic Constraints*, The 31st Annual Congress of the American Romanian Academy of Arts and Sciences, Brasov-Romania, July 31-August 5, 2007.

[8] I. Stroe, P. Parvu, *Holonomic and Nonholonomic Constraints in Dynamics of Multibody Systems*, 7th International DAAAM Baltic Conference Industrial Engineering, Tallin-Estonia, April 22-24, 2010.

[9] I. Stroe, S. Staicu, A. Craifaleanu, *Internal Forces calculus of Compass Robotic Arm using Lagrange Equations*, 11th Symposium on Advanced Space Technologies for Robotics and Automation "ASTRA 2011", ESTEC; Noordwijk, The Nederlands;; 6 pages, April, 12 – 14, 2011.

[10] I. Stroe, A. Craifaleanu, *Generalization of the Lagrange Equations Formalism for Motions with respect to Non-Inertial Reference Frames*, Applied Mechanics and Material, Vol. 656, Trans Tech Publications, Switzerland, pp. 171-180, 2014.

[11] D. N. Dumitriu, C. Secara, *Dynamics of a Planar 3-DOF Manipulator*, SISOM 2010 and Session of the Commission of Acoustics, ISSN 2068-0481, pp. 181-190, Bucharest 27-28 May, 2010.

[12] D. Le Tien, K. Hee-Jun, R. Young-Shick, *Robot manipulator modeling in Matlab-SimMechanics with PD control and online Gravity compensation*, Proceeding of Strategic Technology (IFOST, pp. 446-449), 2010.

[13] L. Sciavicco, B. Siciliano, *Modeling and control of Robot manipulators*, 2nd edition, Springer, London, 378 pages, 2000.

[14] T. V. Nguyen, R. Petre, I. Stroe, *Calculus of axial force in a mechanism using Lagrange equations*, 4th International Workshop on Numerical Modeling in Aerospace Sciences, Incas Bulletin, Vol. 8, Iss. 2, pp. 97-108, 2016.

[15] T.V. Nguyen, R.A. Petre, I. Stroe, *Application of Lagrange Equations for Calculus of Internal Forces in a Mechanism*, U.P.B. Sci. Bull., ISSN 1454-2358, 78, Politehnica Press, Bucharest, pp. 15 – 26, 2016.

[16] T. V. Nguyen, D. Dumitriu, I. Stroe, *Controlling the Motion of a Planar 3-DOF Manipulator using PID controllers*, 5th International Workshop on Numerical Modeling in Aerospace Sciences, Incas Bulletin, Vol. 9, Iss. 4, pp. 91-99, 2017.

[17] T. V. Nguyen, I. Stroe, A. Craifaleanu, R. Petre, D. Dumitriu*, A method for calculus of Internal Forces*, Aerospace Europe 6th CEAS Conference, 16-20 October, 2017.

[18] M. H. Nguyen, V. D. H. Nguyen, T. V. Nguyen, M. T. Nguyen, *Application of Fuzzy and PID Algorithm in Gantry Crane Control*, Journal of Technical Education Science, ISSN 1859-1272, Vol. 44A, pp. 48-53, October 2017.

[19] M. Lazar, N. Pandrea, D. Popa, *An optimal synthesis method of the four-bar planes mechanisms for the imposed trajectories generating*, The Eight IFToMM International Symposium on Theory of Machines and Mechanisms, Vol.1, pp. 159-164, Bucharest 2001.

[20] M. Pandrea, N. Pandrea, D. Popa, *The matrical iterative method and calculation algorithms for the cinematic analyze of spatial mechanisms*, ID: 597 12th IFToMM World Congress, Besancon (France), June 18-21, 2007.